Loss of inhibition in sensorimotor networks in focal hand dystonia

Cecile Gallea, Priyantha Herath, Valerie Voon, Alicja Lerner, John Ostuni, Ziad Saad, Shantalaxmi Thada, Solomon Jeffrey, Silvina G. Horovitz, Mark Hallett

NeuroImage: Clinical 17 (2018) 90–97

Contents lists available at ScienceDirect

NeuroImage: Clinical

journal homepage: www.elsevier.com/locate/ynicl

Loss of inhibition in sensorimotor networks in focal hand dystonia

Cecile Gallea[a,b,*], Priyantha Herath[a], Valerie Voon[a,c], Alicja Lerner[a,d], John Ostuni[e], Ziad Saad[f], Shantalaxmi Thada[g], Jeffrey Solomon[f], Silvina G. Horovitz[a], Mark Hallett[a]

[a] Human Motor Control Section, NINDS, NIH, Bethesda, MD, United States
[b] Institut du Cerveau et de la Moelle (ICM-CRICM), Centre de Neuroimagerie de Recherche (UPMC/INSERM, UMR_975, CNRS 7225), Hôpital de la Pitié Salpétrière, Paris, France
[c] Behavioural and Clinical Neurosciences Institute, University of Cambridge, Cambridge, UK
[d] Center for Drug Evaluation and Research, Food and Drug Agency, Silver Spring, MD, United States
[e] NINDS, NIH, Bethesda, MD, United States
[f] Expert Image Analysis, LLC, Potomac, Maryland, United States
[g] PET, CC, NIH, Bethesda, MD, United States

ARTICLE INFO

Keywords:
Cerebellum
Motor cortex
Focal dystonia
Inhibition
Movement disorder

ABSTRACT

Objective: To investigate GABA-ergic receptor density and associated brain functional and grey matter changes in focal hand dystonia (FHD).

Methods: 18 patients with FHD of the right hand and 18 age and gender matched healthy volunteers (HV) participated in this study. We measured the density of GABA-A receptors using [^{11}C] Flumazenil and perfusion using [^{15}O] H_2O. Anatomical images were also used to measure grey matter volume with voxel-based morphometry (VBM).

Results: In FHD patients compared to HV, the vermis VI of the right cerebellum and the left sensorimotor cortex had a decrease of Flumazenil binding potential (FMZ-BP), whereas the striatum and the lateral cerebellum did not show significant change. Bilateral inferior prefrontal cortex had increased FMZ-BP and an increase of perfusion, which correlated negatively with disease duration. Only the left sensorimotor cortex showed a decrease of grey matter volume.

Interpretation: Impairments of GABAergic neurotransmission in the cerebellum and the sensorimotor cortical areas could explain different aspects of loss of inhibitory control in FHD, the former being involved in maladaptive plasticity, the latter in surround inhibition. Reorganization of the inferior prefrontal cortices, part of the associative network, might be compensatory for the loss of inhibitory control in sensorimotor circuits. These findings suggest that cerebellar and cerebral GABAergic abnormalities could play a role in the functional imbalance of striato-cerebello-cortical loops in dystonia.

1. Introduction

Focal hand dystonia (FHD) is clinically characterized by involuntary muscular co-contraction causing incoordination and abnormal posturing of the hand during skillful movements that are over-trained. A common hypothesis to explain the pathophysiology of FHD is a reduction of inhibitory control over the cortical motor areas that would cause sustained muscle contraction (Beck and Hallett, 2011; Hallett, 2011; Marsden, 1995; Mink, 2003). Yet, there is at present no direct demonstration of what would cause such a phenomenon. In this study, we seek to better understand the pathophysiology of inhibitory control in FHD.

Inhibitory control in the human brain is achieved through the neurotransmitter gamma-aminobutyric acid (GABA). Pharmacological work using Flumazenil, a benzodiazepine antagonist that binds to GABA-A receptors, showed GABAergic impairments in the thalamus and the cerebellum in animal models of dystonia (Ledoux and Lorden, 2002; Zhang et al., 2011; Zhao et al., 2011). GABAergic dysfunctions in the striatum and the cerebellum have been suggested in FHD (Ceballos-Baumann et al., 1995a; Krystkowiak et al., 1998; Lehéricy et al., 1996; Shakkottai et al., 2016). A flumazenil study found GABAergic deficits in the sensorimotor cortex but none in the cerebellum and putamen in dystonic patients (Garibotto et al., 2011). A majority of the patients in this study had DYT1 dystonia and all had impairments affecting several body parts except for two with focal dystonia. DYT1 dystonia differs from FHD, which is typically sporadic, acquired after intensive and

* Corresponding author at: Institut du Cerveau et de la Moelle (ICM), Centre de Neuroimagerie de recherche (CENIR), Hôpital Pitié Salpêtrière, 47, bd de l'hôpital, 75013 Paris, France.
E-mail address: c.gallea-ihu@icm-institute.org (C. Gallea).

http://dx.doi.org/10.1016/j.nicl.2017.10.011
Received 15 May 2017; Received in revised form 5 September 2017; Accepted 10 October 2017
Available online 13 October 2017

repetitive motor practice, and affects a specific type of skillful hand movements.

GABAergic neuromodulation is involved in the fine tuning of brain networks (Popa et al., 2013). It is conceivable that altered GABAergic neuromodulation would be associated with functional abnormalities in the sensorimotor network. For instance, FHD patients are known to have functional impairments in the primary and secondary motor cortices, in the striatum and cerebellum (Wu et al., 2010; Butz et al., 2006; Garraux et al., 2004). Task-related activation studies cannot easily isolate functional changes primarily related to the disease, because they often involve groups with different motor performances or task-induced compensatory mechanisms. Resting state represents a useful tool to isolate disease-related changes, and abnormal resting state activity has been observed in striato-cortical and the cerebello-cortical loops in FHD (Dresel et al., 2014; Hinkley et al., 2013). In addition to functional changes, GABAergic deficits in sensorimotor areas could be associated with structural changes as already found in this patient population (Delmaire et al., 2007; Gibb et al., 1992). Loss of grey matter volume in areas showing GABAergic deficits would suggest that abnormal inhibitory control could be related to neuronal loss.

In a homogeneous patient population of FHD with focal symptoms in the right dominant hand and matching healthy controls, we used a multimodal imaging protocol including (1) Positron Emission Tomography (PET) with flumazenil binding; (2) PET with [^{15}O]-H_2O to investigate cerebral activation of brain areas with abnormal GABAergic receptor density; and (3) MRI voxel-based morphometry to verify whether areas with abnormal GABAergic receptor density would have abnormal grey matter volume. We hypothesize that the functional imbalance of striato-cerebello-cortical loops are due to decreases in inhibition in the contralateral striatum, contralateral sensorimotor cortex, and the ipsilateral cerebellum.

2. Methods

2.1. Subjects

We studied eighteen patients with focal hand dystonia and eighteen healthy volunteers. Patient ages ranged from 24 to 65 years (3 women, 15 men; mean age ± standard deviation = 53.94 ± 12.04 years); eighteen control subjects were matched for age from 22 to 65 years and sex (3 women, 15 men; mean age ± standard deviation = 53.29 ± 12.79 years). All subjects had normal neurologic examinations apart from FHD diagnosis in the patient group. The duration of FHD ranged from 3 to 41 years (mean ± standard deviation = 13.8 ± 9 years). All patients were also evaluated with the Fahn-Marsden scale (FMS, score range from 2 to 4) to assess for the severity and specificity (restricted to the hand) of symptoms. Patients who participated in the study did not present any symptoms at rest so that there was no interference with the scanning procedure. Patients were off any medication affecting the central nervous system during the study and for at least 3 months before the study. Specifically, none of the subjects were on benzodiazepine medication, which binds GABA-A receptors and competes directly with flumazenil for binding; baclofen which binds GABA-B receptors; flunitrazepam, a benzodiazepine receptor agonist; or triazolam, a partial allosteric modulator of GABA-A receptors. All patients had their last injection of botulinum toxin (BoNT) at least 3 months before the study. The study was approved by the Institutional Review Board of the National Institutes of Health. All participants gave their informed consent.

2.2. MRI and PET procedures

For all subjects, high-resolution structural T1-weighted images were acquired for anatomical co-registration with a 3 T GE scanner (9 min, TR = 6.172 ms, TE = 3.2 ms, slice thickness = 1.3 mm, no gap, FOV = 240 × 240 mm^2, 256 × 256 matrix, in-plane resolution = 0.9375 × 0.9375 mm^2). For the PET scan acquisition, participants were scanned using a General Electric Advance Scanner (GE Medical Systems, Waukesha, WI). Images were acquired in axial order (FOV = 150 × 150 mm^2, 35 contiguous slices were acquired, plane separation = 4.25 mm; spatial resolution of raw PET images was 6 to 7 mm full width at half maximum (FWHM)). An 8-min transmission scan for attenuation correction was obtained at the beginning of the session (see Lerner et al., 2007; Lerner et al., 2012). Subject motion during the PET acquisition was corrected with mutual-information registration of each scan timeframe to a standard frame before attenuation correction (Andersson et al., 1995). Based on the calculated motion, the transmission images were resliced and projected for final reconstruction and realignment (matrix size of 256 × 256 matrix, in plane resolution = 2 × 2 mm^2). To minimize head movements during the scans, an individually molded thermoplastic mask was placed on the face and head of each subject. Subjects were instructed to lie still while relaxing with their eyes closed, to think of nothing in particular and not to fall asleep. The entire duration of the PET procedures was two hours, one hour for [^{15}O] H_2O to measure regional cerebral blood flow (rCBF), and one hour for flumazenil to measure GABA-A receptors.

During the first hour, all subjects received 5 intravenous boluses of 10 mCi of [^{15}O] H_2O at 10-minute intervals. The distribution of cerebral radioactivity was measured in a 60-second emission scan after each bolus injection. No arterial line was inserted because of the equivalence in errors in measuring tissue radioactivity and in the calculated rCBF (Herscovitch et al., 1983; Lerner et al., 2007; Lerner et al., 2012). During the second hour, and after the injection of 20 mCi of [^{11}C] flumazenil, 60-min dynamic emission images of the brain were acquired.

2.3. Data analysis

2.3.1. PET

Binding potential images for flumazenil (FMZ-BP) were created using the 2-step version of the simplified reference tissue model (SRTM2) (Wu and Carson, 2002). The input kinetics for the reference tissue were derived from the pons (drawn on each individual's MR image), where the [^{11}C] flumazenil binding is predominantly accounted for by free and non-specifically bound radiotracer (Lerner et al., 2007; Lerner et al., 2012; Millet et al., 2002; Odano et al., 2009). FMZ-BP images were corrected for partial volume effects and grey-white matter ratios on a pixel by pixel basis (Giovacchini et al., 2005). FMZ-BP images (already transformed to MR space) were normalized to the standard Montreal Neurological Institute (MNI) PET template (Ashburner and Friston, 1999) using AFNI (http://afni.nimh.nih.gov/afni, Bethesda, MD), smoothed (FWHM of 10 mm) and analyzed using SPM8 (Wellcome Department of Imaging Neuroscience, UCL, London, UK; http://www.fil.ion.ucl.ac.uk/spm/) implemented in Matlab (Mathworks Inc., Natick, MA). To test our hypothesis, a between group analysis was performed (2 sample *t*-test) to show the brain areas that had a decrease or an increase of FMZ-BP in patients when compared with healthy subjects at the level of the whole brain. Age and sex were included in this analysis as nuisance covariates. An additional region of interest (ROI) analysis was run for contralateral striatal (putamen and caudate nuclei) regions involved in sensorimotor functions using the a-priori masks of the YEB atlas normalized in MNI space (Lehéricy et al., 2006), and ipsilateral cerebellar lobules V,VI and VIII containing a representation of the hand (Schmahmann et al., 1999; Küper et al., 2012; Schlerf et al., 2010).

The image processing and analysis of resting state rCBF levels were performed using Statistical Parametric Mapping SPM8. The images were realigned to the first volume. The resliced volumes were normalized to a standard PET template based on the MNI reference brain in MNI space (Talairach and Tournoux, 1988). Additionally, we used an atlas for the cerebellum (Schmahmann et al., 1999) for the spatial localization of the clusters. The normalized images of 2 ∗ 2 ∗ 2 mm^3

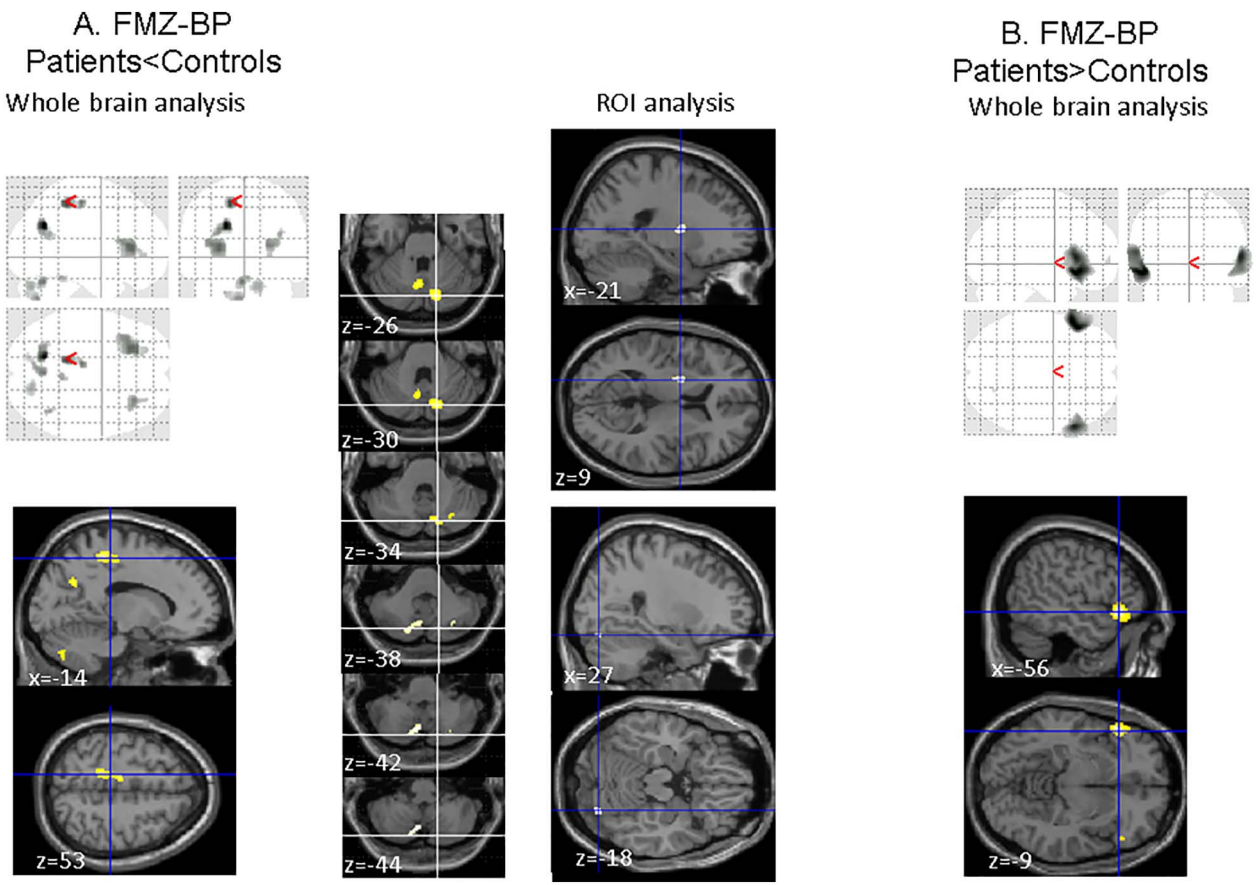

Fig. 1. Results of the two-sample t-test showing the spatial localization of clusters with group difference in flumazenil binding potential (FMZ-BP) ($p < 0.05$, FWE correction at the cluster level). A. Lower flumazenil binding potential in FHD patients compared to controls displayed on a glass brain (upper central view). Clusters localized in the left sensorimotor cortex, and the vermis of the cerebellum are displayed on the canonical brain of SPM. The results of the ROI analysis including the left putamen and the right cerebellar hemisphere (lobule VI) are displayed on the right. B. higher flumazenil binding potential in FHD patients compared to controls displayed on a glass brain (upper view). Clusters localized in the inferior frontal gyri are displayed on the canonical brain of SPM (lower views).

voxels were smoothed with 10 mm FWHM isotropic Gaussian kernel. Global CBF was adjusted to an arbitrary value of 50 (Lerner et al., 2007); an effect of the different global CBF values in different scans was removed by analysis of covariance. A summed PET image (0–10 minute post-injection) was registered to each subject's MRI with a mutual information algorithm and all the PET images were resliced (for more details, see Lerner et al., 2007). We performed a between group analysis (2 sample *t*-test) to show the brain areas that were overactive or underactive in patients when compared with healthy subjects at rest. Second, a regression analysis was performed for the patients to test for possible correlation between individual measures of perfusion and disease duration. Age and sex were incorporated in the design matrix of the regression analysis to remove the variance percentage related to variables of non interest that could interfere with the correlation.

After verification of the normality of data distribution, Pearson correlation was performed between FMZ-BP values and rCBF levels in regions showing a group difference in each previous analysis. Data were extracted averaging the signal in all the voxels included in the significant cluster from the previous group analyses. Since there were several rCBF measures and a single FMZ value per subject, the p-values were adjusted for multiple comparisons using the permutations test (Nichols and Holmes, 2002). We conducted an approximate multivariate permutation test. At each iteration, the max-correlation coefficient was computed to build the sampling distribution. Using this distribution, the corrected p-value was calculated for each correlation coefficient.

2.3.2. Voxel-based morphometry

Images were processed using the VBM8 toolbox (http://dbm.neuro.uni-jena.de/vbm/), of the SPM8 software. Normalized grey matter probability maps were obtained from the T1-weighted images. The processing included denoising (Manjón et al., 2010), partial volume estimation (Tohka et al., 2004) and normalization to the MNI space using Dartel (Ashburner and Friston, 2005). The normalized maps were smoothed with a 10 mm FWHM Gaussian kernel.

In the statistical analysis, the individual smoothed-normalized maps were included in a two-sample *t*-test to perform a group comparison. Age and sex were incorporated in the design matrix to remove the variance percentage related to variables of non-interest that could interfere with group differences. We tested the possible correlation between grey matter volume and individual values of FMZ-BP in areas showing an effect of group in the PET FMZ-BP and the VBM analyses. To do that, we extracted the individual FMZ-BP values in the region of interest (average of all the voxels included in cluster showing a decrease of BP-FMZ in FHD patients for the group analysis) and, within the same region of interest, the individual mean values of grey matter probability maps. For each region of interest, a Pearson correlation was performed (after verification of the normality of data distribution) between individual FMZ-BP values and individual mean values of grey matter probability maps (threshold of significance at $p < 0.05$ corrected for multiple comparisons if needed).

2.3.3. Statistical threshold

We had strong a priori hypotheses on small anatomical regions such as the hand area of the sensorimotor cortex with high inter-individual

Table 1
Anatomical localization of clusters showing group difference in flumazenil binding potential displayed in Fig. 1, and in O^{15}water displayed in Fig. 2. MNI = Montreal Neurological Institute, Ke = number of voxels in the cluster, BA = Brodmann area, L = left, R = right, B = bilateral. Italic font refers to the result of the region of interest analysis (ROI).

Anatomical localization	MNI coordinates of cluster local maxima			T score	Ke
	x	y	z		
FMZ-BP: Patients < healthy volunteers					
L precuneus (BA 7, 31)	− 18	− 62	32	3.73	207
L paracentral lobule (BA 5),	− 14	− 38	56	3.35	189
postcentral gyrus (BA 3),	− 22	− 25	58	3.31	
precentral gyrus (BA 4, 6) (cluster extension in the hand area of the primary motor cortex)					
L insula, inferior frontal operculum	− 26	32	10	3.20	514
L cerebellum (vermis 6, fastigium)	− 2	− 62	− 24	3.05	88
R inferior frontal operculum, inferior frontal gyrus	28	34	12	3.02	156
L cerebellum (lobule 3)	− 6	− 42	− 22	2.92	97
R cerebellum (Crus 1)	16	− 76	− 30	2.81	133
L sensorimotor putamen (ROI analysis)	*− 21*	*− 2*	*9*	*2.01*	*34*
FMZ-BP: Patients > healthy volunteers					
L inferior frontal gyrus (BA 45, 46, 47)	− 50	24	− 8	4.40	527
R inferior frontal gyrus (BA 45, 46, 47)	58	26	6	3.93	477
O^{15}water: Patients > healthy volunteers					
R middle frontal gyrus	46	48	30	8.17	407
R inferior postcentral gyrus, Rolandic operculum (BA 43)	68	− 16	18	8.00	270
B medial orbitofrontal cortex (BA 10)	8	68	− 4	7.76	786
R superior orbitofrontal cortex (BA 11)	16	30	− 22	7.47	1410
R anterior cingulate cortex (BA 24)	4	32	6	6.66	
R anterior putamen and caudate	24	12	− 2	6.53	
L middle frontal gyrus	− 38	48	30	5.70	251
R inferior frontal gyrus (operculum, pars triangularis), superior temporal sulcus	60	14	2	6.58	505
L anterior caudate	− 14	18	0	6.55	207
L inferior frontal gyrus (pars triangularis)	− 44	32	− 14	6.08	652
L middle frontal gyrus (BA 8)	− 44	24	20	6.04	366
L middle temporal pole (BA 38)	− 52	14	− 30	5.87	132
VBM: Patients < healthy volunteers					
L precentral gyrus (BA 6, PMd)	− 28	15	50	3.41	241
L postcentral gyrus (BA 2, 3)	− 20	− 44	77	3.08	274

spatial variability (Yousry et al., 1997). Thus, all the results (FMZ-BP, rCBF and VBM) were considered significant at a statistical threshold of $p < 0.001$ uncorrected at the level of the whole brain (Boecker et al., 2010) with a cluster threshold of 50 contiguous voxels, and at $p < 0.05$ with family wise error (FWE) correction for multiple comparisons at the level of the cluster. For the region of interest analysis involving the contralateral sensorimotor territory of the putamen and caudate, and the ipsilateral sensorimotor lobules of the cerebellum (V, VI, VIII), the results were considered significant at a statistical threshold of $p < 0.05$ with family wise error (FWE) correction for multiple comparisons for the number of considered regions ($n = 5$).

3. Results

3.1. PET FMZ-BP

At the whole-brain level, the two-sample *t*-test showed that patients had a decrease of FMZ-BP in the left dorsal part of the precentral gyrus (PMd), the primary sensorimotor cortex (including the hand area), the left anterior insula, the bilateral vermis VI of the cerebellum (more on the right than on the left; Fig. 1A, Table 1). In the inverse contrast (i.e. HV-FHD), patients showed an increase of FMZ-BP in the bilateral inferior ventral prefrontal cortex compared to controls (Brodmann area 44, 45, 47; Fig. 1B, Table 1).

At the ROI level, the two-sample *t*-test showed that patients had a tendency toward a decrease of FMZ-BP in the left sensorimotor territory of the putamen ($T = 2.01$, $p = 0.04$ uncorrected for multiple comparisons), and in the sensorimotor territory of the cerebellar lobule VI ($T = 1.71$, $p = 0.04$ uncorrected for multiple comparisons). These ROI results did not survive the correction for multiple comparisons.

3.2. PET rCBF

Patients, compared with the healthy volunteers, showed an increase of resting state rCBF in the bilateral inferior and middle frontal gyri (Brodmann area 44, 45, 47), in the orbitofrontal cortex, the anterior cingulate cortex, the right caudate head and the right ventro-anterior part of the putamen. Results are displayed in Fig. 2A and listed in Table 1. Regions showing both an increased FMZ-BP and resting state rCBF are shown in Fig. 2B. Only the left inferior frontal gyrus overlapped in the two modalities. The increase of resting state rCBF in the left inferior frontal gyrus negatively correlated with the FMZ-BP in the right cerebellar vermis and with disease duration (Fig. 2C–D). Such correlation was not observed with the cluster of the sensorimotor cortex, the sensorimotor putamen or the cerebellar lobule VI ($0.28 < p < 0.47$).

3.3. VBM

The regions showing difference of binding potential were defined as regions of interest for the VBM analysis. Only the left sensorimotor cortex corresponding to the hand area and the PMd showed a decrease of grey matter volume (see Fig. 3A). In the sensorimotor cortex, we observed a trend suggesting that the decrease of grey matter volume correlated with the decrease of FMZ-BP (Fig. 3B). None of the other areas with abnormal FMZ-BP had a significant group difference in grey matter volume ($p > 0.001$ uncorrected for multiple comparisons at the level of the whole brain).

4. Discussion

In a patient population with focal right hand dystonia, we verified our hypotheses of an abnormal decrease of GABA-A receptor density in the vermis VI of the right cerebellum and in the left sensorimotor cortex. Bilateral inferior prefrontal cortex had an increase in FMZ-BP and of resting state activity, which correlated negatively with disease duration and the loss of GABA-A receptor density in the cerebellum. Decrease of FMZ-BP in the sensorimotor cortex was accompanied with decrease of grey matter volume, but this was not the case for the cerebellar vermis. These findings seem to indicate that in FHD, the loss of inhibitory control in sensorimotor areas originate in GABA-ergic abnormalities. The loss of inhibitory control is accompanied by cortical reorganization involving the inferior frontal gyrus. These results reinforce the view that despite focal motor symptoms, the pathophysiology of dystonia engages changes in larger associative cortical networks.

Several mechanisms could explain the decrease of GABAergic receptor density in the sensorimotor network: (i) a loss of cells with GABA-A receptors; (ii) decreased number of receptors on the same number of cells; (iii) an identical number of GABAergic receptors but a dysfunctional binding site. In our study, there was a decrease of grey matter volume at the site of decreased FMZ-BP in the sensorimotor cortex confirming the findings of another study (Delmaire et al., 2007), suggesting neuronal loss. This cell loss was however not observed at the

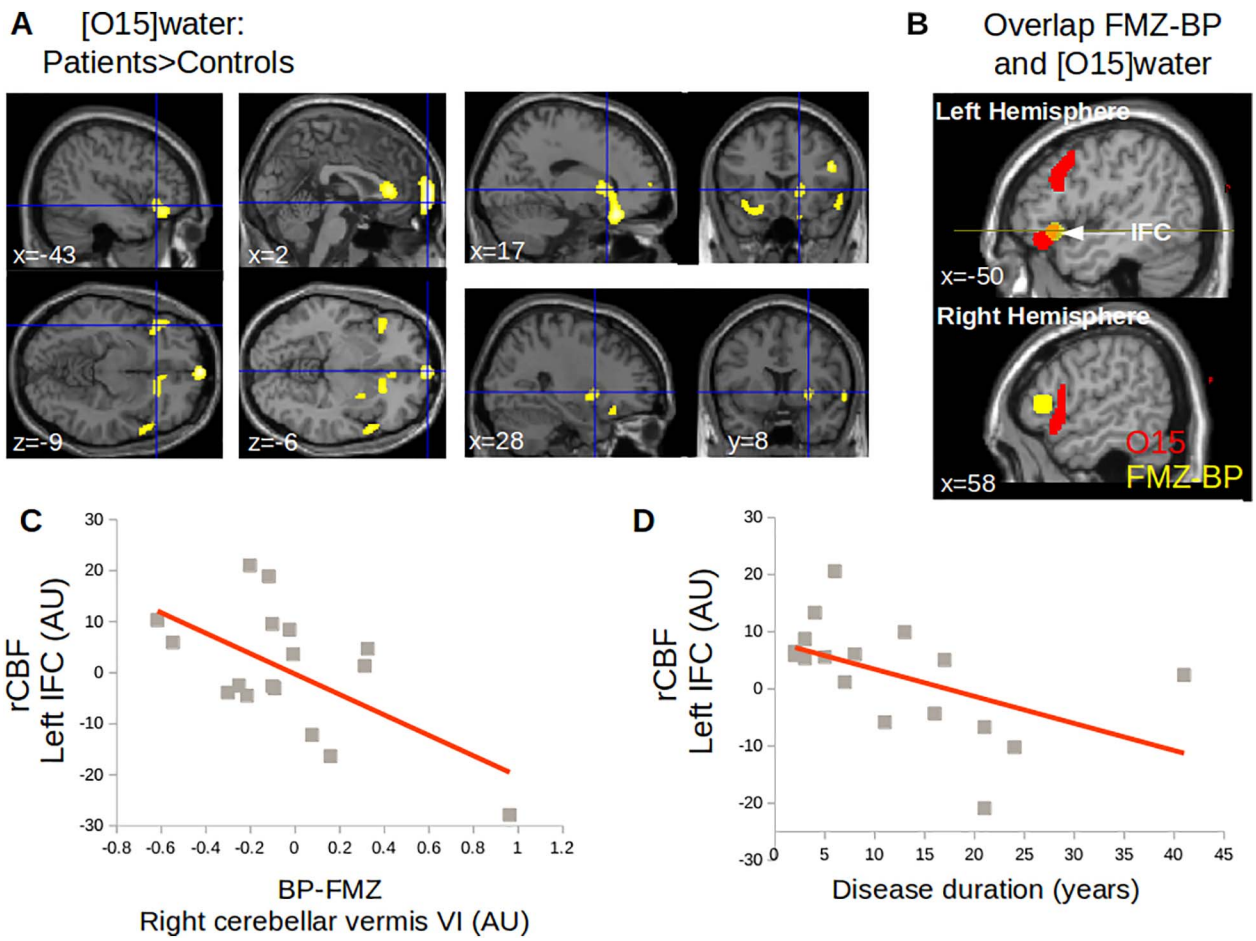

Fig. 2. Results of group comparison of rCBF PET and correlation analyses. A. Inferior prefrontal cortex, and caudate show an increase of rCBF in FHD patients compared to healthy controls ($p < 0.05$ with FWE correction over the whole brain). B. Overlap of areas showing an increase of rCBF and an increase of FMZ-BP, involving only the left prefrontal cortex. C. Correlation between rCBF in the left inferior prefrontal cortex and the FMZ-BP in the right cerebellar vermis ($p = 0.004$, Rho $= -0.54$). D. Correlation between rCBF in the left inferior prefrontal cortex and the disease duration ($p = 0.01$, Rho $= -0.46$). The significance of the correlation takes into account repeated measures (see Methods).

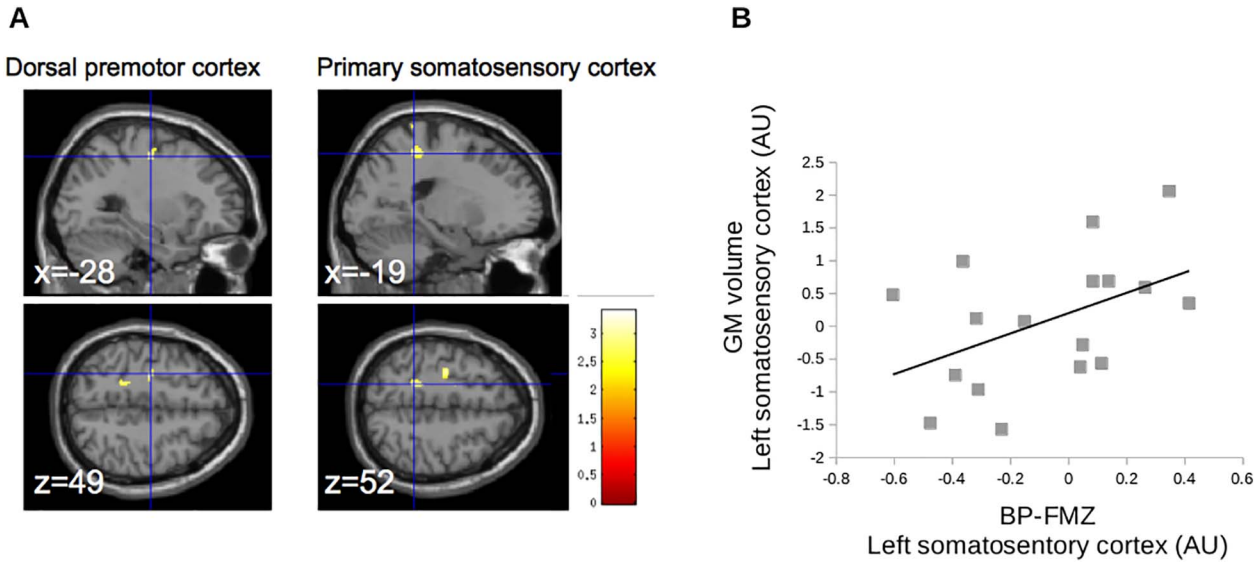

Fig. 3. Results of VBM analysis in regions of interest. A. Decrease of grey matter volume in the precentral gyrus, located in the dorsal premotor cortex (left panels) and the postcentral gyrus (right panels); $p < 0.001$, with FWE correction at the level of the cluster. B. In the left sensorimotor cortex, individual values of grey matter volume tended to correlate with individual values of BP-FMZ ($p = 0.06$, Rho $= 0.46$).

site of the right cerebellar vermis. The absence of change in grey matter volume at that location of GABA-ergic abnormalities however does not preclude the possibility of abnormal morphology. Indeed, synaptic loss or dendritic transections are not fully captured by VBM analyses because of special sensitivity limitations. Moreover, our sample size might be not large enough to detect morphometric changes. This, together with differences in methodology or patient phenotypes, explain the discrepancy found concerning changes of grey matter volume in the primary sensorimotor cortex and the cerebellum, which some found increased (Ramdhani et al., 2014; Garraux et al., 2004), or decreased (Delmaire et al., 2007) or unchanged (Zeuner et al., 2015). Thus, a decrease in the number of GABA-A receptors due to a reduced synthesis of GABA neurotransmitter cannot be ruled out. Indeed, decreased GABA levels were measured in the primary motor cortex of FHD patients compared to control subjects using MR spectroscopy (Levy and Hallett, 2002), although another study failed to confirm it (Herath et al., 2010). Decreases of FMZ-BP could also be due to excessive GABA synthesis which would cause more competition with flumazenil in the synaptic cleft. In that case, it would have to be associated with a dysfunctional binding site.

The reduced grey matter volume and the decrease of FMZ-BP are likely associated with the loss of GABAergic neurons in sensorimotor cortices involved in controlling the symptomatic hand. GABA-ergic abnormalities in the sensorimotor cortex might relate to impairment of specific neurons with somatotopic representations. Previous studies have reported that FHD patients showed somatotopic disorganization in the motor cortex (Weise et al., 2011; Meunier et al., 2001; Nelson et al., 2009). We suggest that a decrease of GABAergic function within M1 and S1 could underlie the changes of somatotopic representation by a larger spread of neuronal excitation. In healthy volunteers, high frequency repetitive somatosensory stimulation modulates short intracortical inhibition within M1 (Rocchi et al., 2017), mediated by GABA-A interneurons (Chen, 2004). Short intracortical inhibition within M1 or between PMd and M1 is reduced in FHD (Currà et al., 2000; Tinazzi et al., 2000; Beck and Hallett, 2011), and interpreted as a loss of surround inhibition. The loss of GABA-A neurons in the sensorimotor cortex could contribute to abnormal interactions between sensory and motor areas, supporting the loss of surround inhibition and the patients' inability to perform individuated finger movement (Moore et al., 2012). To validate this hypothesis, future multimodal studies will have to test whether the individual GABA-A binding potential in the sensorimotor cortex would be related to individual values of short intracortical inhibition in M1.

FMZ-BP in the cerebellum was not found to be abnormal in the previously reported patient population including DYT1 and sporadic dystonia, with symptoms in multiple limbs (Garibotto et al., 2011). Our patient population with homogeneous and focal symptoms affecting the right dominant hand had focal GABA-ergic impairments of the cerebellar vermis. The cerebellar vermis is connected to cortical motor areas and would participate in controlling the anticipatory postural adjustments during hand movement initiation (Diedrichsen et al., 2005). It was speculated that dysfunction of this system may underlie abnormal postural control in dystonia (Coffman et al., 2011). Recently, an abstract report of patients with cervical dystonia showed decreased GABA binding in the cerebellar vermis and the dorsal premotor cortex (Pollard et al., 2016), confirming that this network is relevant for focal dystonia. In accordance with our findings, the cerebellar vermis is also a relevant site to explain dystonic symptoms since microinjection of kainic acid into this structure generates dystonia in mice (Pizoli et al., 2002).

The cerebellum may be one of the primary nodes underlying dystonia (Shakkottai et al., 2016). If that is the case, how would the loss of inhibitory control in the cerebellum affect the cerebello-cortical loop and be related to dystonic symptoms? Defective GABA-ergic neurotransmission in the cerebellum could induce abnormal cerebello-cortical dialog, particularly in the gamma frequency band, and explain abnormal muscular activity. For instance, blockade or inactivation of GABA-ergic neurons of the cerebellum abolishes or decreases gamma rhythms of cerebellar output and of the sensorimotor cortex (Popa et al., 2013; Middleton et al., 2008). The integrity of the GABAergic system also influences neuroplasticity mechanisms, for example in long term potentiation (LTP) of synaptic efficacy (Stefan et al., 2000; Wolters et al., 2003). Patients with FHD have over-reactive LTP-like plasticity (Quartarone et al., 2003), and cerebellar stimulation fails to induce plastic modulation of M1 in this patient population (Hubsch et al., 2013). We suggest that the loss of cerebellar modulation of M1 probably originates in the loss of GABAergic cells in the sensorimotor network.

Neumann et al. (2015) found that the degree of pallido-cerebellar coupling, in the sense that GPi drove the activity of the cerebellum, showed an inverse correlation with dystonic symptom severity. This suggests that striatal dysfunction impacts on cerebellar activation, reducing the communication in striato-cerebellar circuits as disease severity increases. Whether the resulting cerebellar output is adaptive or maladaptive is difficult to say with certainty at this point. Variations of cerebellar-cortical functional connectivity at rest could reflect both an underlying abnormality or compensatory neuroplastic changes of network architecture in focal hand dystonia (Dresel et al., 2014). A compensatory role of the left cerebellar cortex (CrusI) was found during motor sequence learning in DYT1 mutation carriers (Carbon et al., 2011), a structure involved in the early phase of motor learning (Doyon et al., 2003; Floyer-Lea and Matthews, 2005). In the light of these results, GABAergic changes in associative cerebellar structures such as the CrusI could be compensatory or adaptative.

Increased resting state activity of prefrontal regions was observed in our FHD patients. Changes of resting state activity was observed in previous studies using PET (Ceballos-Baumann and Brooks, 1997; Ceballos-Baumann et al., 1997; Ceballos-Baumann et al., 1995a, 1995b; Playford et al., 1998) and fMRI (Bharath et al., 2015; Dresel et al., 2014; Delnooz et al., 2013). In genetic dystonia, increased activation in the inferior frontal gyrus cortex was interpreted as compensatory to sensorimotor loop dysfunction (Carbon et al., 2004; Nakamura et al., 2001). Our results seem to favor this view for FHD: inferior prefrontal cortex has increased GABA-ergic neurotransmission, which correlated negatively with GABA-ergic neurotransmission in the cerebellar vermis and with disease duration. The relationship between GABA-ergic function and dystonic symptoms suggests the existence of plastic changes with time in the inferior frontal gyrus. These findings are intriguing because, despite the focal symptoms, they suggest the existence of complex regulatory systems involving larger networks than the ones involved in sensorimotor integration. The variability of disease severity was small in our patients, which could be a reason why we did not find a correlation with symptom severity. The inferior frontal gyrus is involved in building sensorimotor schemes to adapt finger configuration during grasping tasks (Jeannerod et al., 1995). This area is also involved in the prevention of unwanted movement by ‘calling out’ or compensating for motor areas responsible for the final motor output (Duann et al., 2009; Obeso et al., 2013; Sharp et al., 2010; Swick et al., 2008). Our study raises further evidence that local neurotransmitter contents like GABA relate to functional specialization of brain regions (Greenhouse et al., 2016), which are abnormal in FHD (Gallea et al., 2016).

This study has several limitations. For instance, we found only a tendency toward GABA-ergic abnormalities in the striatum, despite the well-known striatal alterations in this disorder (Marsden et al., 1985; Delmaire et al., 2009; Delnooz et al., 2013). It is also possible that cerebellar interactions with the striatum contribute to the dystonic symptoms through other neurotransmitters. Cerebellar activity can directly influence the dynamics of striatal dopamine (Neychev et al., 2008), and it is known that FHD has striatal dopaminergic impairments (Berman et al., 2013; Karimi et al., 2011). Another limitation is the lack of serial blood sampling for plasma input function to fit compartmental models. However, the modelling technique used in the present study

allows quantifying BP using a reference tissue in which no specific binding of the radioligand occurs, without arterial blood sampling (Lerner et al., 2012). The individual values of BP in the regions of interest were normalized with the BP of the pons, which also cancelled out the influence of individual level of blood concentration. Therefore, the correlations between FMZ-BP and rCBF seem to be likely related to the functional relationship between the changes of GABAergic neurotransmission and perfusion. Last, correlation between symptom severity and FMZ-BP or rCBF could not be evaluated due to the lack of sensitivity of the Burke-Fahn-Marsden scale to task-specific focal hand dystonia and resulted in a narrow range of scores.

Acknowledgements

This study was supported by the NINDS intramural program (including fellowships to CG and VV) and the Fondation pour la Recherche Médicale (FRM, grant to CG). We thank Elaine Considine for patient care and logistics, and the PET department (http://www.cc.nih.gov/pet/) for help with the data acquisition.

Contributions

CG participated in the conception, study design, data analysis and editing;
PH, VV, SGH participated in the study design and editing;
AL, JO, ZS, ST and JF participated in the conception and data analysis;
MH participated in the conception, study design and editing.

References

Andersson, J.L., Vagnhammar, B.E., Schneider, H., 1995. Accurate attenuation correction despite movement during PET imaging. J. Nucl. Med. 36, 670–678.
Ashburner, J., Friston, K.J., 1999. Nonlinear spatial normalization using basis functions. Hum. Brain Mapp. 7, 254–266.
Ashburner, J., Friston, K.J., 2005. Unified segmentation. Neuroimage 26 (3), 839–851 PMID:15955494.
Beck, S., Hallett, M., 2011. Surround inhibition in the motor system. Exp. Brain Res. 210 (2), 165–172.
Berman, B.D., Hallett, M., Herscovitch, P., Simonyan, K., 2013. Striatal dopaminergic dysfunction at rest and during task performance in writer's cramp. Brain 136, 3645–3658.
Bharath, R.D., Biswal, B.B., Bhaskar, M.V., Gohel, S., Jhunjhunwala, K., Panda, R., George, L., Gupta, A.K., Pal, P.K., 2015. Repetitive transcranial magnetic stimulation induced modulations of resting state motor connectivity in writer's cramp. Eur. J. Neurol. 22 (5), 796–805.
Boecker, H., Weindl, A., Brooks, D.J., Ceballos-Baumann, A.O., Liedtke, C., Miederer, M., Sprenger, T., Wagner, K.J., Miederer, I., 2010. GABAergic dysfunction in essential tremor: an 11C-flumazenil PET study. J. Nucl. Med. 51, 1030–1035.
Butz, M., Timmermann, L., Gross, J., Pollok, B., Dirks, M., Hefter, H., et al., 2006. Oscillatory coupling in writing and writer's cramp. J. Physiol. Paris 99, 14–20.
Carbon, M., Ma, Y., Barnes, A., Vijay, Dhawan, Chaly, T., Felice, Ghilardi Maria, et al., 2004. Caudate nucleus: influence of dopaminergic input on sequence learning and brain activation in Parkinsonism. NeuroImage 21, 1497–1507.
Carbon, M., Argyelan, M., Ghilardi, M.F., Mattis, P., Dhawan, V., Bressman, S., Eidelberg, D., 2011. Impaired sequence learning in dystonia mutation carriers: a genotypic effect. Brain 134 (5), 1416–1427.
Ceballos-Baumann, A.O., Brooks, D.J., 1997. Basal ganglia function and dysfunction revealed by PET activation studies. Adv. Neurol. 74, 127–139.
Ceballos-Baumann, A.O., Passingham, R.E., Marsden, C.D., Brooks, D.J., 1995a. Motor reorganization in acquired hemidystonia. Ann. Neurol. 37, 746–757.
Ceballos-Baumann, A.O., Passingham, R.E., Warner, T., Playford, E.D., Marsden, C.D., Brooks, D.J., 1995b. Overactive prefrontal and underactive motor cortical areas in idiopathic dystonia. Ann. Neurol. 37, 363–372.
Ceballos-Baumann, A.O., Sheean, G., Passingham, R.E., Marsden, C.D., Brooks, D.J., 1997. Botulinum toxin does not reverse the cortical dysfunction associated with writer's cramp. A PET study. Brain 120 (Pt 4), 571–582.
Chen, R., 2004. Interactions between inhibitory and excitatory circuits in the human motor cortex. Exp. Brain Res. 154, 1–10.
Coffman, K.A., Dum, R.P., Strick, P.L., 2011 Sep 20. Cerebellar vermis is a target of projections from the motor areas in the cerebral cortex. Proc. Natl. Acad. Sci. U. S. A. 108 (38), 16068–16073.
Currà, A., Romaniello, A., Berardelli, A., Cruccu, G., Manfredi, M., 2000. Shortened cortical silent period in facial muscles of patients with cranial dystonia. Neurology 54, 130–135.
Delmaire, C., Vidailhet, M., Elbaz, A., Bourdain, F., Bleton, J.P., Sangla, S., et al., 2007. Structural abnormalities in the cerebellum and sensorimotor circuit in writer's cramp. Neurology 69, 376–380.
Delmaire, C., Vidailhet, M., Wassermann, D., Descoteaux, M., Valabregue, R., Bourdain, F., Lenglet, C., Sangla, S., Terrier, A., Deriche, R., Lehéricy, S., 2009. Diffusion abnormalities in the primary sensorimotor pathways in writer's cramp. Arch. Neurol. 66, 502–508.
Delnooz, C.C., Pasman, J.W., Beckmann, C.F., van de Warrenburg, B.P., 2013. Task-free functional MRI in cervical dystonia reveals multi-network changes that partially normalize with botulinum toxin. PLoS One 8 (5), e62877 (May 1).
Diedrichsen, J., Verstynen, T., Lehman, S.L., Ivry, R.B., 2005. Cerebellar involvement in anticipating the consequences of self-produced actions during bimanual movements. J. Neurophysiol. 93, 801–812.
Doyon, J., Penhune, V., Ungerleider, L.G., 2003. Distinct contribution of the cortico-striatal and cortico-cerebellar systems to motor skill learning. Neuropsychologia 41, 252–262.
Dresel, C., Li, Y., Wilzeck, V., Castrop, F., Zimmer, C., Haslinger, B., 2014 Nov. Multiple changes of functional connectivity between sensorimotor areas in focal hand dystonia. J. Neurol. Neurosurg. Psychiatry 85 (11), 1245–1252.
Duann, J.R., Ide, J.S., Luo, X., Li, C.S., 2009. Functional connectivity delineates distinct roles of the inferior frontal cortex and presupplementary motor area in stop signal inhibition. J. Neurosci. 29 (32), 10171e9.
Floyer-Lea, A., Matthews, P.M., 2005. Distinguishable brain activation networks for short- and long-term motor skill learning. J. Neurophysiol. 94, 512–518.
Gallea, C., Horovitz, S.G., Ali Najee-Ullah, M., Hallett, M., 2016. Impairment of a parieto-premotor network specialized for handwriting in writer's cramp. Hum. Brain Mapp. http://dx.doi.org/10.1002/hbm.23315. (Jul 28).
Garibotto, V., Romito, L.M., Elia, A.E., Soliveri, P., Panzacchi, A., Carpinelli, A., et al., 2011. In vivo evidence for GABA(A) receptor changes in the sensorimotor system in primary dystonia. Mov. Disord. 26, 852–857.
Garraux, Gaëtan, Bauer, A., Takashi, Hanakawa, Wu, T., Kansaku, K., Mark, Hallett, 2004. Changes in brain anatomy in focal hand dystonia. Ann. Neurol. 55, 736–739.
Gibb, W.R., Kilford, L., Marsden, C.D., 1992. Severe generalised dystonia associated with a mosaic pattern of striatal gliosis. Mov. Disord. 7, 217–223.
Giovacchini, G., Toczek, M.T., Bonwetsch, R., Anto, Bagic, Lang, L., Fraser, C., et al., 2005. 5-HT 1A receptors are reduced in temporal lobe epilepsy after partial-volume correction. J. Nucl. Med. 46, 1128–1135.
Greenhouse, I., Noah, S., Maddock, R.J., Ivry, R.B., 2016. Individual differences in GABA content are reliable but are not uniform across the human cortex. NeuroImage 139, 1–7. http://dx.doi.org/10.1016/j.neuroimage.2016.06.007. (Jun 9).
Hallett, M., 2011. Neurophysiology of dystonia: the role of inhibition. Neurobiol. Dis. 42, 177–184.
Herath, P., Gallea, C., van der Veen, J.W., Horovitz, S.G., Mark, Hallett, 2010. In vivo neurochemistry of primary focal hand dystonia: a magnetic resonance spectroscopic neurometabolite profiling study at 3T. Mov. Disord. 25, 2800–2808.
Herscovitch, P., Markham, J., Raichle, M.E., 1983. Brain blood flow measured with intravenous H2(15)O. I. Theory and error analysis. J. Nucl. Med. 24, 782–789.
Hinkley, L.B., Sekihara, K., Owen, J.P., Westlake, K.P., Byl, N.N., Nagarajan, S.S., 2013. Complex-value coherence mapping reveals novel abnormal resting-state functional connectivity networks in task-specific focal hand dystonia. Front. Neurol. 4, 149.
Hubsch, C., Roze, E., Popa, T., Russo, M., Balachandran, A., Pradeep, S., Mueller, F., Brochard, V., Quartarone, A., Degos, B., Vidailhet, M., Kishore, A., Meunier, S., 2013. Defective cerebellar control of cortical plasticity in writer's cramp. Brain 136, 2050–2062.
Jeannerod, M., Arbib, M.A., Rizzolatti, G., Sakata, H., 1995. Grasping objects: the cortical mechanisms of visuomotor transformation. Trends Neurosci. 18, 314–320.
Karimi, M., Moerlein, S.M., Videen TO, Luedtke, R.R., Taylor, M., Mach, R.H., Perlmutter, J.S., 2011. Decreased striatal dopamine receptor binding in primary focal dystonia: a D2 or D3 defect? Mov. Disord. 26, 100–106.
Krystkowiak, P., Martinat, P., Defebvre, L., Pruvo, J.P., Leys, D., Destée, A., 1998. Dystonia after striatopallidal and thalamic stroke: clinicoradiological correlations and pathophysiological mechanisms. J. Neurol. Neurosurg. Psychiatry 65, 703–708.
Küper, M., Thürling, M., Stefanescu, R., Maderwald, S., Roths, J., Elles, H.G., et al., 2012. Evidence for a motor somatotopy in the cerebellar dentate nucleus–an FMRI study in humans. Hum. Brain Mapp. 33, 2741–2749.
LeDoux, M.S., Lorden, J.F., 2002. Abnormal spontaneous and harmaline-stimulated Purkinje cell activity in the awake genetically dystonic rat. Exp. Brain Res. 145, 457–467.
Lehéricy, S., Vidailhet, M., Dormont, D., Piérot, L., Chiras, J., Mazetti, P., et al., 1996. Striatopallidal and thalamic dystonia. A magnetic resonance imaging anatomoclinical study. Arch. Neurol. 53, 241–250.
Lehéricy, S., Bardinet, E., Tremblay, L., Van de Moortele, P.F., Pochon, J.B., Dormont, D., Kim, D.S., Yelnik, J., Ugurbil, K., 2006. Motor control in basal ganglia circuits using fMRI and brain atlas approaches. Cereb. Cortex 16, 149–161.
Lerner, A., Bagic, A., Boudreau, E.A., Hanakawa, T., Pagan, F., Mari, Z., et al., 2007. Neuroimaging of neuronal circuits involved in tic generation in patients with Tourette syndrome. Neurology 68, 1979–1987.
Lerner, A., Bagic, A., Simmons, J.M., Mari, Z., Bonne, O., Xu, B., Kazuba, B., Herscovitch, P., Carson, R.E., Murphy, D.L., Drevets, W.C., Hallett, M., 2012. Widespread abnormality of the GABA-ergic system in Tourette syndrome. Brain.
Levy, L.M., Hallett, Mark, 2002. Impaired brain GABA in focal dystonia. Ann. Neurol. 51, 93–101.
Manjón, J.V., Tohka, J., Robles, M., 2010. Improved estimates of partial volume coefficients from noisy brain MRI using spatial context. NeuroImage 53, 480–490.
Marsden, C.D., 1995. Psychogenic problems associated with dystonia. Adv. Neurol. 65, 319–326.
Marsden, C.D., Obeso, J.A., Zarranz, J.J., Lang, A.E., 1985. The anatomical basis of

symptomatic hemidystonia. Brain 108 (Pt 2), 463–483.
Meunier, S., Garnero, L., Ducorps, A., Mazières, L., Lehéricy, S., du Montcel, S.T., et al., 2001. Human brain mapping in dystonia reveals both endophenotypic traits and adaptive reorganization. Ann. Neurol. 50, 521–527.
Middleton, S.J., Racca, C., Cunningham, M.O., Traub, R.D., Monyer, H., Knöpfel, T., Schofield, I.S., Jenkins, A., Whittington, M.A., 2008. High-frequency network oscillations in cerebellar cortex. Neuron 58 (5), 763–774.
Millet, P., Graf, C., Buck, A., Walder, B., Ibanez, V., 2002. Evaluation of the reference tissue models for PET and SPECT benzodiazepine binding parameters. NeuroImage 17, 928–942.
Mink, J.W., 2003. The basal ganglia and involuntary movements: impaired inhibition of competing motor patterns. Arch. Neurol. 60, 1365–1368.
Moore, R.D., Gallea, C., Horovitz, S.G., Hallett, M., 2012. Individuated finger control in focal hand dystonia: an fMRI study. NeuroImage 61, 823–831.
Nakamura, T., Ghilardi, M.F., Mentis, M., Dhawan, V., Fukuda, M., Hacking, A., et al., 2001. Functional networks in motor sequence learning: abnormal topographies in Parkinson's disease. Hum. Brain Mapp. 12, 42–60.
Nelson, A.J., Blake, D.T., Chen, R., 2009. Digit-specific aberrations in the primary somatosensory cortex in Writer's cramp. Ann. Neurol. 66 (2), 146–154.
Neumann, W.J., Jha, A., Bock, A., Huebl, J., Horn, A., Schneider, G.H., Sander, T.H., Litvak, V., Kühn, A.A., 2015. Cortico-pallidal oscillatory connectivity in patients with dystonia. Brain 138 (7), 1894–1906.
Neychev, V.K., Fan, X., Mitev, V.I., Hess, E.J., Jinnah, H.A., 2008. The basal ganglia and cerebellum interact in the expression of dystonic movement. Brain 131, 2499–2509.
Nichols, T.E., Holmes, A.P., 2002. Nonparametric permutation tests for functional neuroimaging: a primer with examples. Hum. Brain Mapp. 15 (1), 1–25.
Obeso, I., Cho, S.S., Antonelli, F., Houle, S., Jahanshahi, M., Ko, J.H., Strafella, A.P., 2013. Stimulation of the pre-SMA influences cerebral blood flow in frontal areas involved with inhibitory control of action. Brain Stimul. 6 (5), 769–776. http://dx.doi.org/10.1016/j.brs.2013.02.002.
Odano, I., Halldin, C., Karlsson, P., et al., 2009. [18F]flumazenil binding to central benzodiazepine receptor studies by PET—quantitative analysis and comparisons with [11C]flumazenil. NeuroImage 45, 891–902.
Pizoli, C.E., Jinnah, H.A., Billingsley, M.L., Hess, E.J., 2002. Abnormal cerebellar signaling induces dystonia in mice. J. Neurosci. 22, 7825–7833.
Playford, E.D., Passingham, R.E., Marsden, C.D., Brooks, D.J., 1998. Increased activation of frontal areas during arm movement in idiopathic torsion dystonia. Mov. Disord. 13, 309–318.
Pollard, R., Shelton, E., Koo, P., Berman, B., 2016. GABA-A receptor binding is abnormal in cervical dystonia (P1.030). Neurology 86 (16 Supplement), P1.030 (April 5, Abstract).
Popa, D., Spolidoro, M., Proville, R.D., Guyon, N., Belliveau, L., Léna, C., 2013. Functional role of the cerebellum in gamma-band synchronization of the sensory and motor cortices. J Neurosci. 33 (15), 6552–6556. http://dx.doi.org/10.1523/JNEUROSCI.5521-12.2013.
Quartarone, A., Bagnato, S., Rizzo, V., Siebner, H.R., Dattola, V., Scalfari, A., et al., 2003. Abnormal associative plasticity of the human motor cortex in writer's cramp. Brain 126, 2586–2596.
Ramdhani, R.A., Kumar, V., Velickovic, M., Frucht, S.J., Tagliati, M., Simonyan, K., 2014. What's special about task in dystonia? A voxel-based morphometry and diffusion weighted imaging study. Mov. Disord. 29 (9), 1141–1150. http://dx.doi.org/10.1002/mds.25934. (Aug).
Rocchi, L., Erro, R., Antelmi, E., Berardelli, A., Tinazzi, M., Liguori, R., Bhatia, K., Rothwell, J., 2017. High frequency somatosensory stimulation increases sensorimotor inhibition and leads to perceptual improvement in healthy subjects. Clin. Neurophysiol. 128 (6), 1015–1025.
Schlerf, J.E., Verstynen, T.D., Ivry, R.B., Spencer, R.M.C., 2010. Evidence of a novel somatopic map in the human neocerebellum during complex actions. J. Neurophysiol. 103, 3330–3336.
Schmahmann, J.D., Doyon, J., McDonald, D., Holmes, C., Lavoie, K., Hurwitz, A.S., et al., 1999. Three-dimensional MRI atlas of the human cerebellum in proportional stereotaxic space. NeuroImage 10, 233–260.
Shakkottai, V.G., Batla, A., Bhatia, K., Dauer, W.T., Dresel, C., Niethammer, M., Eidelberg, D., Raike, R.S., Smith, Y., Jinnah, H.A., Hess, E.J., Meunier, S., Hallett, M., Fremont, R., Khodakhah, K., LeDoux, M.S., Popa, T., Gallea, C., Lehericy, S., Bostan, A.C., Strick, P.L., 2016. Current opinions and areas of consensus on the role of the cerebellum in dystonia. Cerebellum 16 (2), 577–594. http://dx.doi.org/10.1007/s12311-016-0825-6. (Oct 12, Review).
Sharp, D.J., Bonnelle, V., De Boissezon, X., Beckmann, C.F., James, S.G., Patel, M.C., et al., 2010. Distinct frontal systems for response inhibition, attentional capture, and error processing. Proc. Natl. Acad. Sci. U. S. A. 107 (13), 6106e11.
Stefan, K., Kunesch, E., Cohen, L.G., Benecke, R., Classen, J., 2000. Induction of plasticity in the human motor cortex by paired associative stimulation. Brain 123 (Pt 3), 572–584.
Swick, D., Ashley, V., Turken, A.U., 2008. Left inferior frontal gyrus is critical for response inhibition. BMC Neurosci. 9, 102.
Talairach, J., Tournoux, P., 1988. Co-planar Stereotactic Atlas of the Human Brain: 3-Dimensional Proportional System, An Approach to Cerebral Imaging Stuttgart. George Thieme Verlag.
Tinazzi, M., Priori, A., Bertolasi, L., Frasson, E., Mauguière, F., Fiaschi, A., 2000. Abnormal central integration of a dual somatosensory input in dystonia. Evidence for sensory overflow. Brain 123 (Pt 1), 42–50.
Tohka, J., Zijdenbos, A., Evans, A., 2004. Fast and robust parameter estimation for statistical partial volume models in brain MRI. NeuroImage 23, 84–97.
Weise, D., Schramm, A., Beck, M., Reiners, K., Joseph, Classen, 2011. Loss of topographic specificity of LTD-like plasticity is a trait marker in focal dystonia. Neurobiol. Dis. 42, 171–176.
Wolters, A., Sandbrink, F., Schlottmann, A., Erwin, Kunesch, Katja, Stefan, Cohen Leonardo, G., et al., 2003. A temporally asymmetric Hebbian rule governing plasticity in the human motor cortex. J. Neurophysiol. 89, 2339–2345.
Wu, Y., Carson, R.E., 2002. Noise reduction in the simplified reference tissue model for neuroreceptor functional imaging. J. Cereb. Blood Flow Metab. 22, 1440–1452.
Wu, C.C., Fairhall, S.L., McNair, N.A., Hamm, J.P., Kirk, I.J., Cunnington, R., et al., 2010. Impaired sensorimotor integration in focal hand dystonia patients in the absence of symptoms. J. Neurol. Neurosurg. Psychiatry 81, 659–665.
Yousry, T.A., Schmid, U.D., Alkadhi, H., Schmidt, D., Peraud, A., Buettner, A., et al., 1997. Localization of the motor hand area to a knob on the precentral gyrus. A new landmark. Brain 120 (Pt 1), 141–157.
Zeuner, K.E., Knutzen, A., Granert, O., Götz, J., Wolff, S., Jansen, O., Dressler, D., Hefter, H., Hallett, M., Deuschl, G., van Eimeren, T., Witt, K., 2015. Increased volume and impaired function: the role of the basal ganglia in writer's cramp. Brain Behav. 5 (2), e00301. http://dx.doi.org/10.1002/brb3.301. (Feb).
Zhang, L., Yokoi, F., Jin, Y.H., DeAndrade, M.P., Hashimoto, K., Standaert, D.G., Li, Y., 2011. Altered dendritic morphology of Purkinje cells in Dyt1 ΔGAG knock-in and purkinje cell-specific Dyt1 conditional knockout mice. PLoS One 6 (3), e18357.
Zhao, Y., Sharma, N., LeDoux, M.S., 2011. The DYT1 carrier state increases energy demand in the olivocerebellar network. Neuroscience 177, 183–194 (Epub 2011 Jan 14).